

## TEM investigation of potassium-calcium feldspar inclusions in Bøggild plagioclase

TAKESHI HOSHI AND TOKUHEI TAGAI

Mineralogical Institute, Graduate School of Science, University of Tokyo, Hongo, Bunkyo-ku, Tokyo 113, Japan

### ABSTRACT

Potassium-calcium feldspar inclusions in a Bøggild plagioclase were investigated by analytical high-resolution transmission electron microscopy (HRTEM), and the formation process of these inclusions is considered based on the Al-Si ordering scheme in ternary feldspar system. Nanometer-scale chemical analyses and selected-area electron diffraction (SAED) patterns show that the rims of the inclusions consist of lamellar intergrowths of potassium feldspar ( $C\bar{1}$  symmetry) and anorthite ( $P\bar{1}$  symmetry), whereas the core is unexsolved potassium feldspar ( $C\bar{1}$  symmetry). Potassium feldspar and anorthite in the inclusions share the crystallographic orientation of the host Bøggild plagioclase. High-resolution lattice images indicate coherent interfaces between the inclusions and the host Bøggild plagioclase and the phases in the inclusions. The results indicate a unique formation process of potassium-calcium feldspar inclusions in a ternary feldspar: crystallization of host labradorite  $\rightarrow$  precipitation of potassium feldspar  $\rightarrow$  decomposition of Bøggild exsolution lamellae  $\rightarrow$  growth of anorthite on the rims of potassium feldspar inclusions. Potassium-calcium feldspar inclusions may be found in Bøggild and other plagioclase, and they have the potential to give constraints on thermal histories of K-rich plagioclase.

### INTRODUCTION

Microstructural observations of potassium-sodium-calcium feldspars provide information about the feldspar ternary system. These phase relationships have the potential to constrain the thermal histories of metamorphic and igneous rocks. For this reason, synthetic potassium-calcium feldspars have been studied extensively to estimate thermodynamic properties and structural information (Nekvasil 1994; Kroll et al. 1986; Fuhrman and Lindsley 1988; Nekvasil and Carroll 1993). Kay (1978) investigated microtextures of experimentally ion-exchanged potassium-calcium feldspar using transmission electron microscopy (TEM). The author determined the orientation of exsolution lamellae and discussed the formation of potassium-calcium feldspar lamellae with respect to antiperthite textures and Bøggild exsolution lamellae of a plagioclase from an anorthosite complex (Kay 1977). It is known that Bøggild exsolution lamellae occur in plagioclases with An contents ranging between  $An_{48 \pm 3}$  and  $An_{58 \pm 3}$  and with Or components greater than 1.6 mol% (Nissen et al. 1967). They have also been reported in  $An_{49}Ab_{51}Or_0$  (Carpenter et al. 1985). Most feldspars showing Bøggild exsolution lamellae are derived from high-grade metamorphic environments, typically of Precambrian age (Smith 1983). Fuhrman and Lindsley (1988) stated that exsolved K-rich feldspars in plagioclases, which affect the original composition of plagioclase, should be taken into account when we consider thermal histories of plagioclases.

Several phases are known in plagioclase and alkali

feldspar. In feldspar, the reflections in the diffraction patterns from these phases are conventionally named  $a$ ,  $b$ ,  $c$ ,  $d$ , and  $e$  (see Smith 1974). The following notation for reflections is commonly used:

$a$ reflections	$h + k = \text{even}, l = \text{even}$
$b$ reflections	$h + k = \text{odd}, l = \text{odd}$
$c$ reflections	$h + k = \text{even}, l = \text{odd}$
$d$ reflections	$h + k = \text{odd}, l = \text{even}$
$e$ reflections	satellites around $b$ reflections

The  $a$  reflections are observed in all feldspars and are related to the average structure with space-group symmetry  $C\bar{1}$ . The  $b$  reflections are observed in calcic plagioclase and are related to  $I\bar{1}$  anorthite. The  $c$  and  $d$  reflections can only be observed in the range  $An_{90}$ - $An_{100}$  and belong to  $P\bar{1}$  anorthite. The  $e$  reflections, satellite reflections of  $b$  reflections, are characteristic of intermediate plagioclase ( $An_{20}$ - $An_{70}$ ) and are divided into  $e_1$  ( $> An_{50}$ ) and  $e_2$  ( $< An_{50}$ ).

Tagai and Hoshi (1995) showed that K in plagioclases from Ylämma, Finland, is segregated into inclusions of potassium-calcium feldspar that are several hundreds of nanometers in diameter. SAED patterns generated from the inclusions and the host plagioclase suggested that the crystallographic orientations of the potassium-calcium feldspar inclusions and the host Bøggild plagioclase were common and that inclusions show structure similar to that of  $P\bar{1}$  anorthite.

In this study, the microtextures of the inclusions were investigated using HRTEM combined with nanometer-

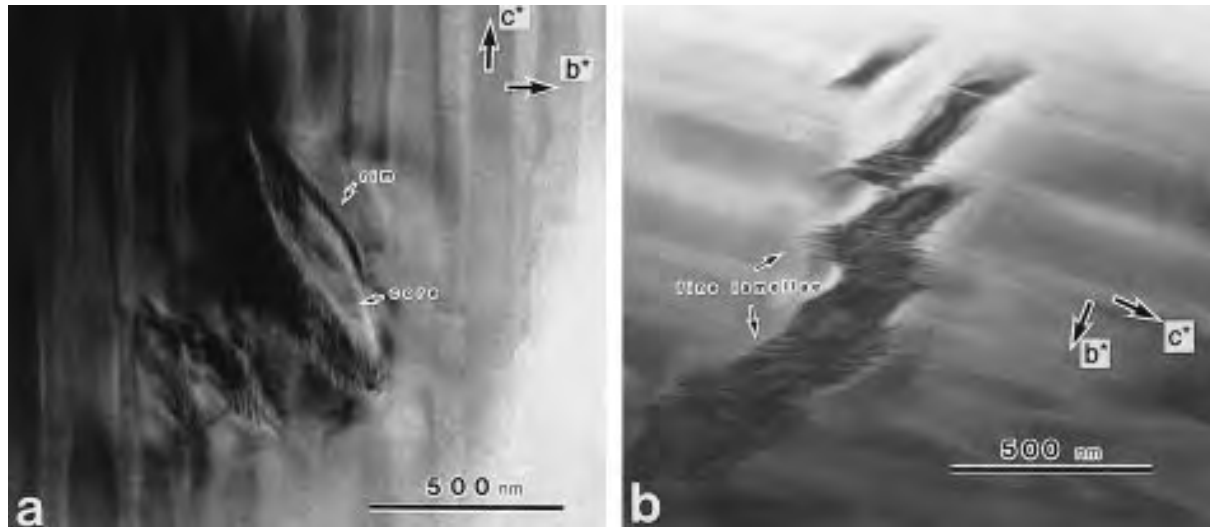


**FIGURE 1.** Transmission electron micrographs. (a) An inclusion cutting across Bøggild exsolution lamellae. Two distinct regions, rim and core, are observed. In the rim region, periodic alternating lamellar structure with linear boundaries is observed. (b) Fine lamellar structure is observed nearly at the boundaries of Bøggild exsolution lamellae.

scale chemical analyses. We report crystallographic properties and interface structures of natural potassium-calcium feldspar inclusions in a Bøggild plagioclase and discuss their formation process.

#### SAMPLES AND EXPERIMENTAL METHODS

A single crystal ( $\sim 3 \times 3 \times 3$  cm<sup>3</sup>) of an iridescent Bøggild plagioclase from Ylämaa, Finland, was selected for the present study. The specimen shows complex interference colors well known as labradorescence, varying from blue to yellow. Hoshi et al. (1996) showed that this was due to the presence of  $160 \pm 10$  nm wide Ca-rich lamellae (Ab<sub>38.7</sub>An<sub>60.1</sub>Or<sub>1.2</sub>) and  $60 \pm 10$  nm Na-rich lamellae (Ab<sub>51.0</sub>An<sub>46.8</sub>Or<sub>2.2</sub>) approximately parallel to (010). Antiperthite textures were not observed in the specimen.

The yellow part of the specimen (Ab<sub>39.6</sub>An<sub>56.9</sub>Or<sub>3.5</sub>; Hoshi et al. 1996) was prepared as an oriented thin section normal to [100] and then thin foils were made for TEM observations by ion-beam milling. The microtextures of the inclusions were investigated using JEOL JEM 2010 and HITACHI HF2000 TEMs operated at an accelerating voltage of 200 keV. Both TEMs are equipped with EDS and KEVEX SIGMA analysis systems.

### RESULTS

#### TEM observations of microtextures of potassium-calcium feldspar inclusions

In each few hundred square micrometer-sized regions of the TEM specimens, we observed inclusions a few hundred nanometers in diameter and a few micrometers in length that cut across the Bøggild exsolution lamellae. The inclusions usually consist of two regions: a rim region exhibiting a lamellar structure and a core region without any distinct texture (Fig. 1a). In some inclusions the lamellar structure was observed better between core

regions and narrower Bøggild lamellae (Fig. 1b). The traces of the boundaries of fine lamellae in the inclusions are either approximately perpendicular to [0.13.2] or [059] when the specimen was viewed down [100] of the host Bøggild plagioclase. The lamellae were generally 5–10 nm wide.

#### Chemical composition of potassium-calcium feldspar inclusions

To clarify the chemical compositions of the rim and the core regions of the inclusions, chemical analyses were obtained using a spot size of  $\sim 2$  nm. It was difficult to determine quantitatively the chemical composition of each lamellar phase within the rim region because few X-rays are generated because of the low beam current and because the area of the analysis may be larger than the individual lamellae. However, the semi-quantitative analysis shows that the rim region includes two phases, specifically K-rich alkali feldspar (denoted as potassium feldspar; Fig. 2a) and anorthite (Fig. 2b). The core region was identified as potassium feldspar (Fig. 2c).

#### Electron diffraction data

Electron diffraction patterns were obtained from inclusions and the host Bøggild plagioclase with the incident beam parallel to [100] of the host Bøggild plagioclase. Figure 3a, which was obtained from an inclusion and the host Bøggild plagioclase, shows elongated *a*, sharp *b* and *c* reflections, very weak *d* reflections, and *e* reflections. Figure 3b, obtained only from the host Bøggild plagioclase, shows sharp *a* and *e* reflections. Figure 3c, obtained only from the lamellar structure of a rim region, shows strong *a* reflections, accompanied by weaker *a* reflections (*x* in Fig. 3c), sharp *b* and *c* reflections, and very weak *d* reflections. The *a* reflections often showed diffuse

streaks. The strong  $a$  and additional weak  $a$  reflections indicate that the lamellar structure of the rim region consists of two structures with slightly different lattice constants. Where lamellae are regularly spaced, the reflections from the rim region were accompanied by satellite reflections, sometimes with diffuse streaks (Fig. 3d). Figure 3e, obtained from the core region, shows only sharp  $a$  reflections. These results indicate that two feldspars with different cell parameters contribute to the diffraction patterns of the inclusion; potassium feldspar and anorthite. Potassium feldspar gives  $a$  reflections and anorthite gives  $a$ ,  $b$ ,  $c$ , and  $d$  reflections. Diffuse streaks of  $a$  reflections observed in Figure 3a are due to the nonperiodic stacking of alternating lamellae. The host Bøggild plagioclase, two phases in the rim region, and the core region show almost the same crystallographic orientation.

#### High-resolution lattice fringe images of the interfaces

High-resolution lattice fringe images were obtained from the rim region, core region, and the host plagioclase. Figure 4a shows interfaces between the host plagioclase and the inclusion rim and between the inclusion rim and core. In this case the rim region is very narrow and the two alternating phases were not clearly observed. Figure 4b shows the interfaces between the two lamellae in the rim region. Figure 4a and 4b indicate that interfaces are coherent. The slight change in orientation of the fringes across the lamellae is attributed to the small difference in lattice constants of each phase (Fig. 4a and 4b).

### DISCUSSION

#### Structure of the potassium-calcium feldspar inclusion

Chemical analyses and electron diffraction patterns show that the inclusions consist of potassium feldspar and anorthite. Lamellar structure was generally observed in the rims of inclusions (Fig. 1a and 1b). From the results of the chemical analyses (Fig. 2a and 2b) and the diffraction patterns (Fig. 3c), it can be concluded that the rim regions consist of two phases, potassium feldspar with  $C\bar{1}$  symmetry and anorthite with  $P\bar{1}$  symmetry. In the core region, only sharp  $a$  reflections were observed (Fig. 3e), and the chemical composition was determined to be nearly  $KAlSi_3O_8$  (Fig. 2c). Therefore, the core regions consist of a single phase of potassium feldspar with  $C\bar{1}$  symmetry. The interfaces between each phase in the inclusions and between the inclusions and the host plagioclase are coherent despite small differences in the cell constants of anorthite, potassium feldspar, and the Bøggild plagioclase phases.

#### Formation of potassium-calcium feldspar inclusions

We make the assumption that the exsolution process occurs in a nonaqueous environment and the process that requires the highest activation energy occurs at the highest temperature and thus occurs first during cooling of the labradorite. After crystallization of the labradorite, the precipitation of the potassium feldspar inclusion occurs because of the presence of a wide miscibility gap in the

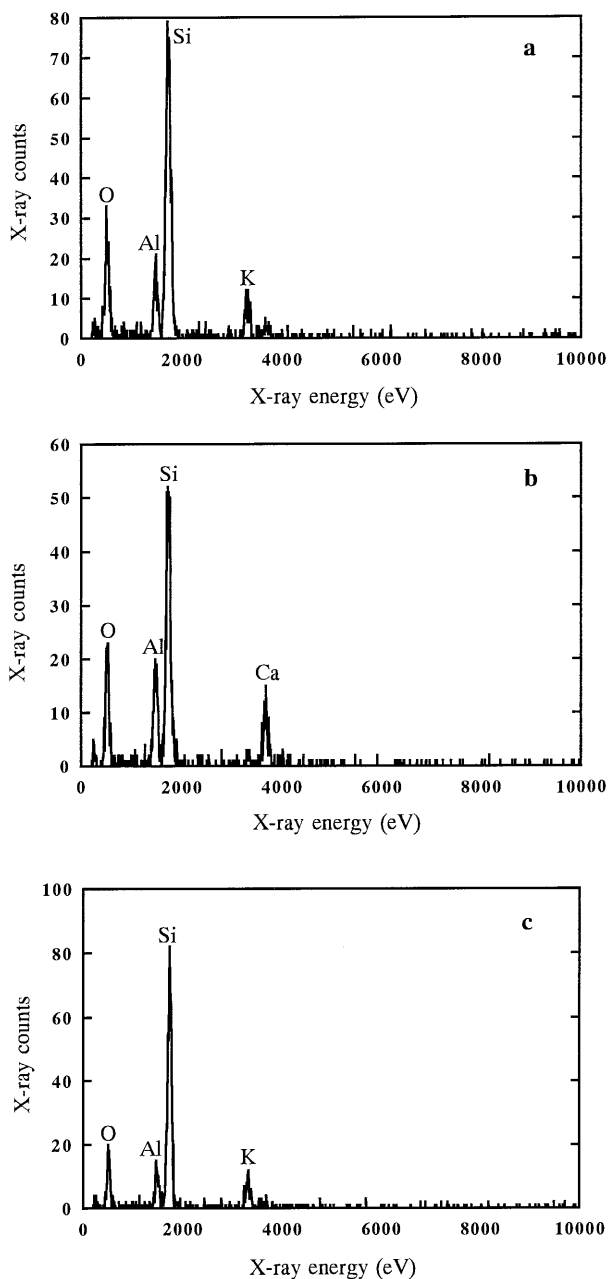


FIGURE 2. The results of qualitative chemical analyses of two phases of rim region (a, b) and core region (c).

ternary system. This segregation is driven by the large alkali ions and by Al-Si ordering as in the plagioclase binary system. This is considered the most energetic exsolution process because of the long-range exchange of Al and Si required for the nucleation and growth of the potassium feldspar inclusion. The temperature range for nucleation and growth of the potassium feldspar inclusion is 700–800 °C for  $Or_{3.5}$  ternary labradorite (Fig. 1 of Nekvasil 1994). The second-most energetic process is assumed to be the short-range exchange of Al and Si re-

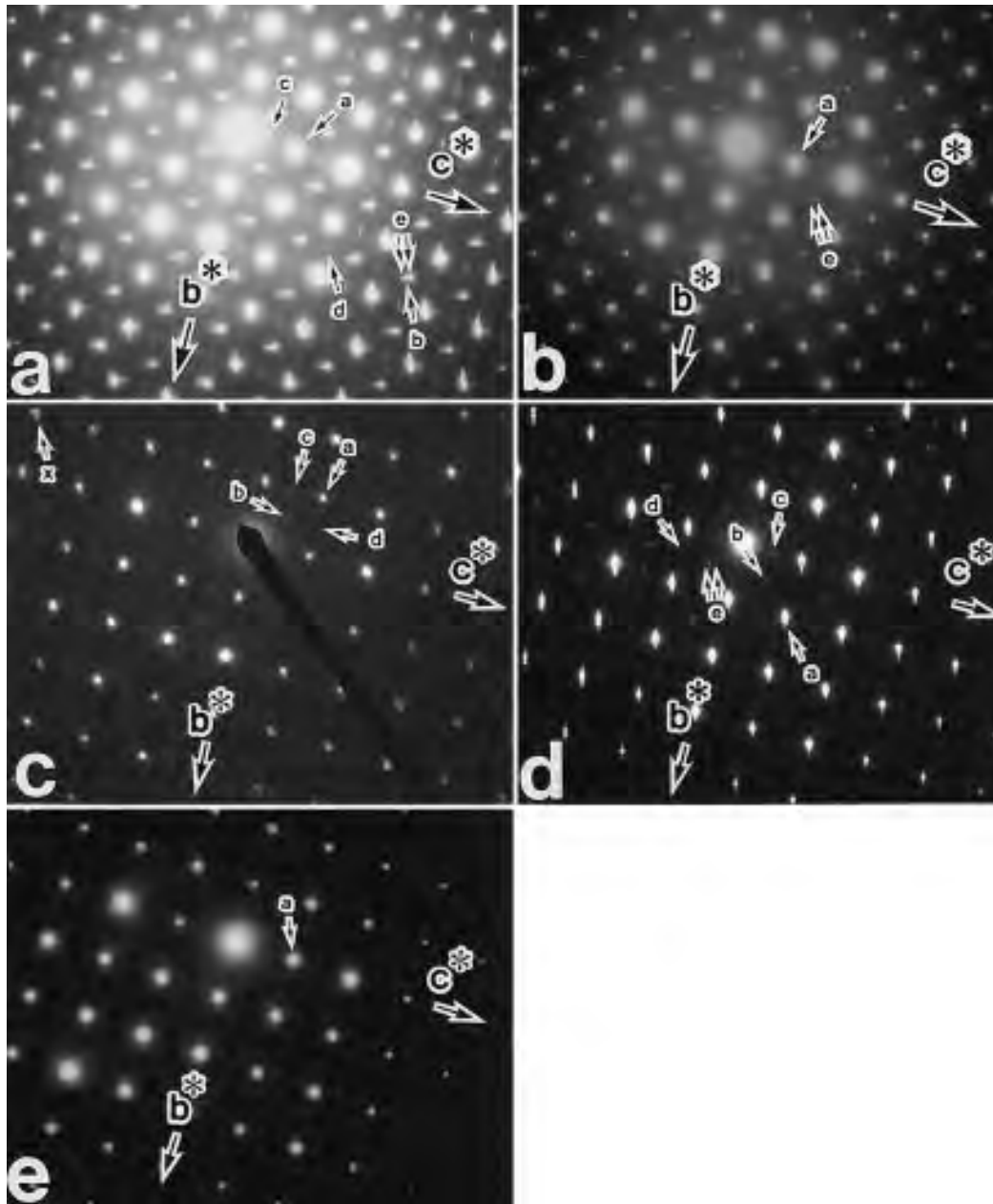


FIGURE 3. Electron diffraction patterns obtained from (a) inclusion and host Bøggild plagioclase, (b) host Bøggild plagioclase, (c) rim region of the inclusion, (d) rim region of the inclusion (periodic lamellae), and (e) core region of the inclusion.

quired to form the Bøggild lamellae and the fine lamellae at the rim of the potassium feldspar inclusion. According to the phase diagrams of Carpenter (1994), Bøggild exsolution lamellae of the present chemical composition may be produced at 700–800 °C, prior to formation of potassium-calcium feldspar inclusions. After the decomposition of labradorite into Bøggild lamellae, the Ca-rich lamellae underwent ordering from  $C\bar{1} \rightarrow I\bar{1} \rightarrow e_1$ , and the Ca-poor lamellae from  $C\bar{1} \rightarrow e_1$  or  $e_2$  (Carpenter 1994).

It is necessary to consider the detailed distribution of K, Na, Ca, Al, and Si in the inclusions and the surround-

ing plagioclase. Kay (1977) noted that the Ca and Al contents of the plagioclase at the contact with the K-rich phase were higher than that of the surrounding plagioclase. She attributed this to the slow rate of Al-Si diffusion required to remove the anorthite component from the K-rich phase zone. Conversely, Kay (1977) reported no concentration of Na in plagioclase at the margin of the K-rich phase and explained this by noting that exchange of albite for the potassium feldspar component does not require Al-Si diffusion.

This slow rate of Al-Si diffusion suggests that the an-

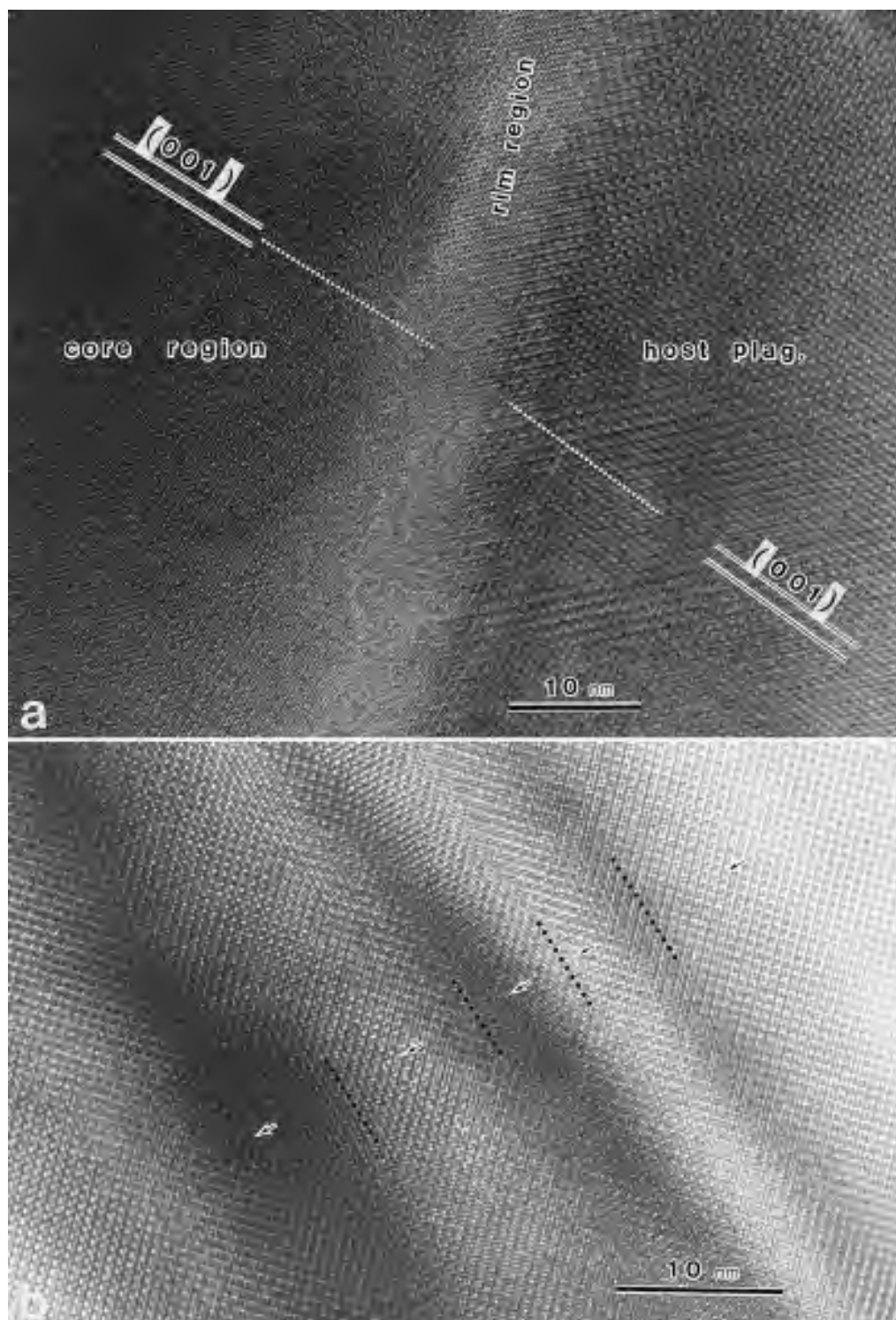


**FIGURE 4.** High-resolution lattice images. (a) Interfaces of rim, core, and host Bøggild plagioclase. Rim region is very narrow. The (001) fringes slightly change their orientation through interfaces. (b) Interfaces of two phases in the rim region. The orientation of (011) fringes parallel to the arrows changes slightly in each phase.

orthite component could be concentrated at the margins of the K-rich phase in Ylämma plagioclase. At the Ca- and Al-enriched rim of the potassium feldspar inclusion,  $I\bar{I}$  anorthite forms between the potassium feldspar inclusion and both sets of the exsolution lamellae in the host Bøggild plagioclase. The anorthite then undergoes the  $I\bar{I} \rightarrow P\bar{I}$  transition at a much lower temperature. This leaves a rim with intergrown  $P\bar{I}$  anorthite and  $C\bar{I}$  potassium feldspar. In some cases (Fig. 1b) the fine lamellae of the rim region were observed only between Ca-poor Bøggild lamellae and the inclusion. We suggest that the excess amount of Ca and Al was similar to that in the Ca-rich Bøggild lamellae; therefore the anorthite formed only between the Ca-poor Bøggild lamellae and the potassium feldspar inclusion.

At the present time, it is not known how common potassium-calcium feldspar inclusions are in plagioclases. Plagioclases in several meteorites include high-K regions (e.g., Yamaguchi et al. 1994). If characterized by TEM, potassium-calcium feldspar inclusions, such as those characterized here, may be found in these and other plagioclases.

#### ACKNOWLEDGMENTS

The authors are grateful to T. Kamino, Hitachi Co. Ltd., for assistance with the analytical electron microscopy. We thank H. Fuess, T.H. Darmstadt, for useful discussions. A review by J. Banfield, University of Tokyo, was very helpful. G.L. Nord Jr., U.S. Geological Survey, also reviewed the entire manuscript and improved our interpretation. TEM observations were carried out in the Electron Microbeam Analysis Facility of the Mineralogical Institute, University of Tokyo.

#### REFERENCES CITED

- Carpenter, M.A. (1994) Subsolidus phase relations of the plagioclase feldspar solid solution. In I. Parsons, Ed., *Feldspars and their reactions* (NATO ASI Series C 421), p. 221–269. Kluwer Academic Publishers, Dordrecht.
- Carpenter, M.A., McConnell, J.D.C., and Navrotsky, A. (1985) Enthalpies of ordering in the plagioclase feldspar solid solution. *Geochimica et Cosmochimica Acta*, 49, 947–966.
- Fuhrman, M.L. and Lindsley, D.H. (1988) Ternary-feldspar modeling and thermometry. *American Mineralogist*, 73, 201–215.
- Hoshi, T., Tagai, T., and Suzuki, M. (1996) Investigations on Bøggild intergrowth of intermediate plagioclase by high resolution transmission electron microscopy. *Zeitschrift für Kristallographie*, 211, 879–883.
- Kay, S.M. (1977) The origin of antiperthite in anorthositic. *American Mineralogist*, 62, 905–912.
- (1978) Exsolution in potassium-calcium feldspars: experimental evidence and relationship to antiperthites and Bøggild lamellae. *American Mineralogist*, 63, 136–142.
- Kroll, H., Schmiemann, I., and von Colln, G. (1986) Feldspar solid solutions. *American Mineralogist*, 71, 1–16.
- Nekvasil, H. (1994) Ternary feldspar/melt equilibria: a review. In I. Parsons, Ed., *Feldspars and their reactions* (NATO ASI Series C 421), p. 195–219. Kluwer Academic Publishers, Dordrecht.
- Nekvasil, H. and Carroll, W.J. (1993) Experimental constraints on the high-temperature termination of the anhydrous 2 feldspar + L curve in the feldspar system at 11.3 kbar. *American Mineralogist*, 78, 601–606.
- Nissen, H.U., Eggmann, H., and Laves, F. (1967) Shiller and submicroscopic lamellae of labradorite: A preliminary report. *Schweizerische Mineralogische und Petrographische Mitteilungen*, 47, 289–302.
- Smith, J.V. (1974) X-ray diffraction techniques. In J.V. Smith, Ed., *Feldspar minerals, I. Crystal structures and physical properties*, p. 179–197. Springer-Verlag, Heidelberg.
- (1983) Phase equilibria of plagioclase. In *Mineralogical Society of America Reviews in Mineralogy*, 2, 223–239.
- Tagai, T. and Hoshi, T. (1995) A new phase of natural feldspar,  $An_{100-x}$ ,  $X \approx 50$ . *Proceedings of the Japan Academy*, 71(B), 2, 72–74.
- Yamaguchi, A., Takeda, H., Bogard, D.D., and Garrison, D. (1994) Textural variations and impact history of the Millbillillie eucrite. *Meteoritics*, 29, 237–245.

MANUSCRIPT RECEIVED OCTOBER 4, 1996

MANUSCRIPT ACCEPTED JULY 11, 1997